

Magnetic Susceptibilities and Mössbauer Spectra of $\text{Sr}_{2-x}\text{La}_x\text{FeO}_{4-\delta}$ ($0 \leq x \leq 0.5$)

Yukio Hinatsu¹, Keitaro Tezuka, and Masaaki Inamura

Division of Chemistry, Graduate School of Science, Hokkaido University, Sapporo 060-0810, Japan

and

Nobuyuki M. Masaki

Japan Atomic Energy Research Institute, Tokai-mura, Ibaraki 319-1195, Japan

Received December 18, 1998; in revised form April 6, 1999; accepted April 22, 1999

Solid solutions $\text{Sr}_{2-x}\text{La}_x\text{FeO}_{4-\delta}$ ($0 \leq x \leq 0.5$) with the K_2NiF_4 -type structure have been prepared, and their magnetic susceptibilities have been measured in the temperature range between 4.2 and 300 K. Substitution of the La ion for the Sr site considerably weakens the antiferromagnetic transition of Sr_2FeO_4 , and it finally disappears in $\text{Sr}_{1.6}\text{La}_{0.4}\text{FeO}_{4-\delta}$. Below the magnetic transition temperatures, magnetic susceptibilities measured under zero-field cooled and field cooled conditions indicate the formation of a spin-glass state. Mössbauer spectra for $\text{Sr}_{1.9}\text{La}_{0.1}\text{FeO}_{4-\delta}$ at room temperature and at 9 K have been measured, and the spectra at 9 K show the presence of magnetic hyperfine interaction of Fe^{4+} ions; there is no charge disproportionation of $\text{Fe}^{4+} \rightarrow \text{Fe}^{3+} + \text{Fe}^{5+}$, even below the magnetic transition temperature. © 1999 Academic Press

INTRODUCTION

Iron in the tetravalent oxidation state is rarely found in complex oxides because it requires strongly oxidizing conditions to prepare them. Perovskite-type oxides ABO_3 , where A is a divalent ion (e.g., Ca, Sr), accommodate tetravalent metal ions at the B site of the crystal. The B -site ions sit at the center of the octahedron formed by six oxygen ions.

Although the number of the perovskite-type oxides with the tetravalent iron is not so large, the magnetic properties of such complex oxides attract our attention. CaFeO_3 and SrFeO_3 exhibit contrasting electronic and magnetic proper-

ties. SrFeO_3 crystallizes with a perfect cubic perovskite structure with no evidence of a structural distortion found above 4 K (1), and Mössbauer data on this material show the iron to exist as $+4$ ions at all temperatures (2). On one hand, below 134 K, SrFeO_3 orders antiferromagnetically with a helical spin structure (3). On the other hand, CaFeO_3 crystallizes with a tetragonally distorted perovskite structure (4). The Mössbauer spectrum measured below room temperature, consisting of a close doublet, has been interpreted as a combined signal resulting from the simultaneous presence of Fe^{3+} and Fe^{5+} ions. When CaFeO_3 is cooled below the Néel temperature, the two different iron types are clearly visible in the Mössbauer spectrum as two magnetically hyperfine split sextets.

As for the other oxygen-stoichiometric complex oxides with iron in the tetravalent oxidation state, there exist Sr_2FeO_4 and $\text{Sr}_3\text{Fe}_2\text{O}_7$. Both of these form a Ruddlesden–Popper-type crystal structure; i.e., the basic units are regular FeO_6 octahedra which are connected via common corners to form two-dimensional iron–oxygen layers (5). $\text{Sr}_3\text{Fe}_2\text{O}_7$ can be considered a Ruddlesden–Popper phase with a 1:1 intergrowth of Sr_2FeO_4 and perovskite SrFeO_3 (6). Both Sr_2FeO_4 and $\text{Sr}_3\text{Fe}_2\text{O}_7$ are semiconductors and order antiferromagnetically at 60 K (7–9) and 110 K (8, 10, 11), respectively. On one hand, the Mössbauer spectrum of $\text{Sr}_3\text{Fe}_2\text{O}_7$ is interpreted in terms of a disproportionation, $\text{Fe}^{4+} \rightarrow \text{Fe}^{3+} + \text{Fe}^{5+}$ (8, 11), although neutron diffraction measurements show a single crystallographic iron site (8). On the other hand, the Mössbauer spectra of Sr_2FeO_4 show a single Fe^{4+} site in the paramagnetic phase, but a complicated distribution of Fe^{4+} sites in the antiferromagnetic phase, indicating the presence of at least four magnetically different Fe^{4+} sites (8, 9).

¹To whom correspondence should be addressed.

To elucidate the electronic state of Fe^{4+} in solids, we focus our attention on the magnetic properties of solid solutions $\text{Sr}_{2-x}\text{La}_x\text{FeO}_4$. Takeda *et al.* (7) obtained the solid solutions $\text{Sr}_{2-x}\text{La}_x\text{FeO}_4$ in an oxygen-flowing atmosphere and refined their crystal structures by the Rietveld method, assuming space group $I4/mmm$. The FeO_6 octahedron in the Sr_2FeO_4 shows almost cubic symmetry, and it becomes elongated along the c axis with the La substitution for Sr.

In this study, we have prepared solid solutions $\text{Sr}_{2-x}\text{La}_x\text{FeO}_{4-\delta}$ ($x = 0-0.5$) and measured their detailed magnetic susceptibilities in the temperature range between 4.2 and 300 K and Mössbauer spectra of $\text{Sr}_{1.9}\text{La}_{0.1}\text{FeO}_{4-\delta}$ at room temperature and at 9 K.

EXPERIMENTAL

1. Sample Preparation

All samples, $\text{Sr}_{2-x}\text{La}_x\text{FeO}_{4-\delta}$ ($x = 0, 0.1, 0.2, 0.3, 0.4,$ and 0.5), were prepared by the conventional ceramic method using starting materials SrO, La_2O_3 , and Fe_2O_3 . Before use, La_2O_3 was dried in air at 1000°C for a day. These starting materials were weighed in the correct ratios, mixed well in an agate mortar, and then pressed into pellets. The pellets were heated under a flowing oxygen atmosphere at 650°C (for $x = 0$ and 0.1), 850°C (for $x = 0.2$ and 0.3), or 1150°C (for $x = 0.4$ and 0.5) for 48 h with interval grindings and then slowly cooled to room temperature in the furnace to obtain the oxygen-stoichiometric compounds.

2. X-Ray Diffraction Analysis

X-ray diffraction profiles of the powdered samples were obtained with a Rigaku RINT 2000 diffractometer using monochromatized $\text{CuK}\alpha$ radiation.

3. Magnetic Susceptibility Measurements

Magnetic susceptibility measurements were made using a SQUID magnetometer (Quantum Design MPMS). Susceptibility-temperature curves for each sample were measured under both the ZFC (zero field-cooled) and FC (field-cooled) conditions. The former was measured on heating the sample to 300 K after zero-field cooling to 4.2 K, applying a field of 1000 G. The latter was measured on cooling from 300 to 4.2 K at 1000 G.

4. Mössbauer Spectrum Measurements

The Mössbauer spectra were measured with a conventional transmission Mössbauer spectrometer operating in the constant acceleration mode. Absorbers were prepared of finely ground $\text{Sr}_{1.9}\text{La}_{0.1}\text{FeO}_{4-\delta}$ which was weighed to give optimum signal to noise and mixed with carbon to ran-

domize the orientations of the microcrystals. A source of up to 100 mCi of ^{57}Co in Rh was used and the spectrometers were calibrated using α -iron at room temperature. The spectra at 9 K were measured with an Oxford flow cryostat.

RESULTS AND DISCUSSION

In this study, we tried to prepare solid solutions of $\text{Sr}_{2-x}\text{La}_x\text{FeO}_4$ with a K_2NiF_4 -type structure in the x range from 0 to 0.5. The results of the X-ray diffraction measurements show that Sr_2FeO_4 and $\text{Sr}_{1.9}\text{La}_{0.1}\text{FeO}_{4-\delta}$ crystallize in the single phase, but the samples with $x \geq 0.2$ contain $\text{Sr}_{3-x}\text{La}_x\text{Fe}_2\text{O}_7$ as an impurity (the molar ratio is ca. 5%). This is probably due to a high-temperature reaction which causes the decomposition of Sr_2FeO_4 into $\text{Sr}_3\text{Fe}_2\text{O}_7$ and SrO (12). The tetragonal lattice parameters a and c of $\text{Sr}_{2-x}\text{La}_x\text{FeO}_4$ are basically consistent with those reported previously (7), and the value of c increases with the lanthanum concentration, while a does not change with it.

Figure 1 shows the temperature dependence of the magnetic susceptibilities for Sr_2FeO_4 and $\text{Sr}_{2-x}\text{La}_x\text{FeO}_{4-\delta}$ solid solutions. Sr_2FeO_4 shows the paramagnetic-antiferromagnetic transition at 58 K, which corresponds to the previous studies (7-9). $\text{Sr}_{1.9}\text{La}_{0.1}\text{FeO}_{4-\delta}$ also shows the antiferromagnetic transition at ca. 29 K. It is found that the substitution of only 5% of La for Sr (corresponding to $x = 0.1$) considerably weakens the peak of antiferromagnetic ordering in the susceptibility vs temperature curve and lowers the magnetic transition temperature. The antiferromagnetic transition is still found even for the $\text{Sr}_{1.7}\text{La}_{0.3}\text{FeO}_{4-\delta}$ solid solution. The transition finally disappears in $\text{Sr}_{1.6}\text{La}_{0.4}\text{FeO}_{4-\delta}$. Since the samples with $x \geq 0.2$ contain several molar percents of $\text{Sr}_{3-x}\text{La}_x\text{Fe}_2\text{O}_{7-\delta}$, such paramagnetic impurity may affect the magnetic properties of $\text{Sr}_{2-x}\text{La}_x\text{FeO}_{4-\delta}$. The inset of Fig. 1 shows the detailed temperature dependence of the magnetic susceptibilities for Sr_2FeO_4 and $\text{Sr}_{1.9}\text{La}_{0.1}\text{FeO}_{4-\delta}$. In the susceptibilities of Sr_2FeO_4 , we have found the existence of a small divergence between ZFC and FC magnetic susceptibilities below 20 K. For the magnetic susceptibility of $\text{Sr}_{1.9}\text{La}_{0.1}\text{FeO}_{4-\delta}$, the most striking feature is the dramatic difference between ZFC and FC magnetic susceptibilities below the magnetic transition temperature. The ZFC susceptibilities decrease with decreasing temperature, while the FC susceptibilities increase with decreasing temperature, which indicates the existence of a spin-glass state in this solid solution. The generation of the Fe^{3+} ion by the substitution of a La^{3+} ion for the Sr^{2+} site introduces disorder and modifies the delicate balance between ferro- and antiferromagnetic interactions, which results in the formation of the frustration state, preventing the development of long-range magnetic ordering. The divergence of magnetic susceptibility between ZFC and FC is also found in other $\text{Sr}_{2-x}\text{La}_x\text{FeO}_4$ solid solutions with $x \geq 0.2$.

Figure 2 shows the Mössbauer spectra of $\text{Sr}_{1.9}\text{La}_{0.1}\text{FeO}_{4-\delta}$ measured at room temperature (298 K) and 9 K. In the spectrum at 298 K (Fig. 2a), the quadrupole splitting does not appear. This result is different from the case of Sr_2FeO_4 of which the Mössbauer spectrum shows the quadrupole splitting (8, 9). In this solid solution, some Fe^{3+} ions are formed by the substitution of La^{3+} ions for the Sr^{2+} sites. Both the Fe^{3+} and Fe^{4+} ions contribute to its magnetic properties. The Mössbauer parameters for $\text{Sr}_{1.9}\text{La}_{0.1}\text{FeO}_{4-\delta}$ are listed in Table 1 and the fitting results are shown in Fig. 2. The ratio of the Fe^{3+} ion is estimated to be 29% from the relative intensity of Fe^{3+} and Fe^{4+} signals. Therefore, the chemical formula for this solid solution is $\text{Sr}_{1.9}\text{La}_{0.1}\text{Fe}_{0.71}^{4+}\text{Fe}_{0.29}^{3+}\text{O}_{3.91}$, indicating some oxygen deficiency. A very small amount of a Fe^{3+} sextet due to unreacted $\alpha\text{-Fe}_2\text{O}_3$ is also found in the Mössbauer spectra. At 9 K, the spectra show complex magnetic hyperfine structures (Fig. 2b). The magnetic hyperfine lines in the range from -5.5 to $+6.5$ mm/s are very similar to those found in the spectra of Sr_2FeO_4 measured below its magnetic transition temperature (8, 9). The Mössbauer study of $\text{Sr}_2\text{FeO}_{4-\delta}$ reveals

complex behavior in the two-dimensional sheets. The observation of, at least, four magnetically inequivalent sites within the planes is unique. We consider that in this $\text{Sr}_{1.9}\text{La}_{0.1}\text{FeO}_{4-\delta}$, there exist four magnetically inequivalent Fe^{4+} sites and that at least four hyperfine split sextets are required to give a reasonable fit to the experimental spectrum (Fig. 2b). This supports the interpretation of the low-temperature Mössbauer data in terms of a single chemical shift as the Fe^{4+} ions are all chemically equivalent but differ only in their relationship to the orientation of the magnetic field. The existence of the hyperfine lines due to the Fe^{4+} ion indicates that no charge disproportionation ($\text{Fe}^{4+} \rightarrow \text{Fe}^{3+} + \text{Fe}^{5+}$) occurs, even at low temperatures. The Mössbauer parameters obtained in this study are listed in Table 1. All four components for the Fe^{4+} ion have the same value of the isomer shift, $\delta = 0.12$ mm/s, corresponding to an Fe^{4+} charge state. The difference in isomer shifts between the 298 and the 9.2 K spectra is due to a second-order Doppler shift. The isomer shifts for the Fe^{3+} ion are 0.32 and 0.44 mm/s, which are reasonable for this charge state.

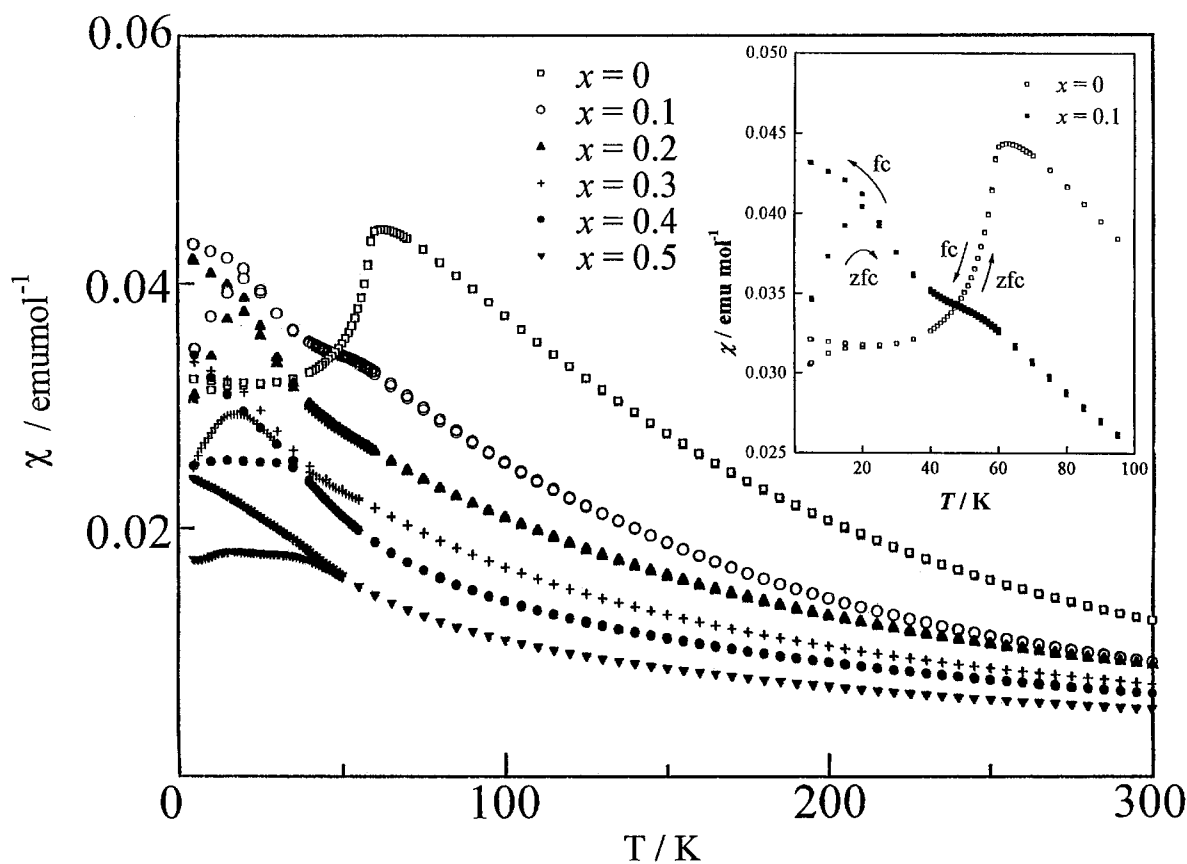


FIG. 1. Temperature dependence of magnetic susceptibilities for $\text{Sr}_{2-x}\text{La}_x\text{FeO}_{4-\delta}$ solid solutions. Below magnetic transition temperatures, the divergence between the ZFC and FC magnetic susceptibilities has been observed for any solid solution. Inset shows the detailed magnetic susceptibility vs temperature curves of Sr_2FeO_4 and $\text{Sr}_{1.9}\text{La}_{0.1}\text{FeO}_{4-\delta}$ at low temperatures.

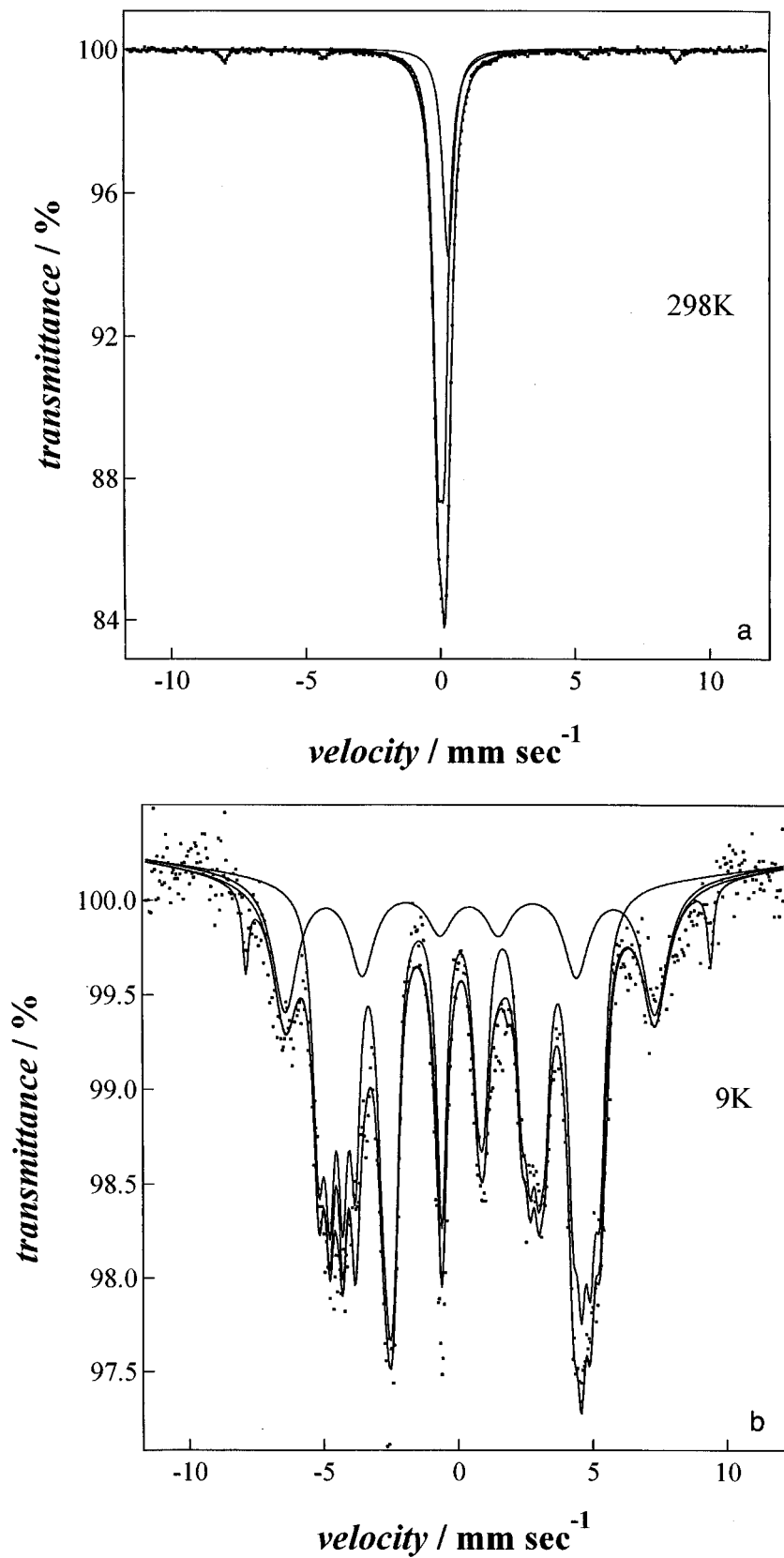


FIG. 2. Mössbauer spectra of Sr_{1.9}La_{0.1}FeO_{4-δ} at 298 K (a) and at 9 K (b). Solid lines correspond to fitting, assuming four magnetically inequivalent Fe⁴⁺ sites and coexisting of Fe³⁺ ions. Mössbauer parameters are given in Table 1.

TABLE 1
Mössbauer Parameters for $\text{Sr}_{1.9}\text{La}_{0.1}\text{FeO}_{4-\delta}$

$T(\text{K})$		298	9		
Fe^{4+}	δ (mm/s)	0.05	δ (mm/s)	0.12	
	Q.S. (mm/s)	0.25	1 Q.S. (mm/s)	-0.17	
	$\Gamma_{1/2}$ (mm/s)	0.38	B_{hf} (T)	32.6	
	area (%)	71	δ (mm/s)	0.12	
			2 Q.S. (mm/s)	-0.12	
			B_{hf} (T)	30.1	area (%)
			δ (mm/s)	0.12	74
			3 Q.S. (mm/s)	0.04	
			B_{hf} (T)	27.6	
			δ (mm/s)	0.12	
			4 Q.S. (mm/s)	0.20	
			B_{hf} (T)	25.2	
Fe^{3+}	δ (mm/s)	0.32	δ (mm/s)	0.44	
	Q.S. (mm/s)	0.004	Q.S. (mm/s)	0.03	area (%)
	$\Gamma_{1/2}$ (mm/s)	0.48	B_{hf} (T)	42.8	26
	area (%)	29			

Note. δ = isomer shift; Q.S. = quadrupole splitting; B_{hf} = magnetic hyperfine field; $\Gamma_{1/2}$ = half-width.

REFERENCES

1. J. B. MacChesney, R. C. Sherwood, and J. F. Potter, *J. Chem. Phys.* **43**, 1907 (1965).
2. Y. Takeda, K. Kanno, T. Takeda, O. Yamamoto, M. Takano, N. Nakanishi, and Y. Bando, *J. Solid State Chem.* **63**, 237 (1986).
3. T. Takeda, Y. Yamaguchi, and H. Watanabe, *J. Phys. Soc. Jpn.* **33**, 967 (1972).
4. Y. Takeda, S. Naka, M. Takano, T. Shinjo, T. Takeda, and M. Shimada, *Mater. Res. Bull.* **13**, 61 (1978).
5. S. E. Dann, D. B. Currie, and M. T. Weller, *J. Solid State Chem.* **92**, 237 (1991).
6. C. Brissi, *Ann. Chim. (Rome)* **51**, 1399 (1961).
7. Y. Takeda, K. Imayoshi, N. Imanishi, O. Yamamoto, and M. Takano, *J. Mater. Chem.* **4**, 19 (1994).
8. S. E. Dann, M. T. Weller, D. B. Currie, M. F. Thomas, and A. D. Al-Rawwas, *J. Mater. Chem.* **3**, 1231 (1993).
9. P. Adler, *J. Solid State Chem.* **108**, 275 (1994).
10. J. B. MacChesney, H. J. Williams, R. C. Sherwood, and J. F. Potter, *Mater. Res. Bull.* **1**, 113 (1966).
11. P. Adler, *J. Solid State Chem.* **130**, 129 (1997).
12. S. E. Dann, M. T. Weller, and D. B. Currie, *J. Solid State Chem.* **97**, 179 (1992).